doi:10.1017/S1431927616005699
Microsc. Microanal. 22 (Suppl 3), 2016

Bandgap State Mapping via Valence-Loss EELS at Grain Boundaries in Non-Stoichiometric $Pr_xCe_{1-x}O_{2-\delta}$

William J. Bowman[1,2], Eva Sediva[2], Jennifer L.M. Rupp[2], Peter A. Crozier[1]

1. School for the Engineering of Matter, Transport and Energy, Arizona State University, Tempe, AZ, USA
2. Electrochemical Materials Group, ETH Zürich, Zürich, Switzerland

We recently reported the enhancement of grain boundary electrical conductivity in polycrystalline $Gd_xCe_{1-x}O_{2-\delta}$ solid solution resulting from the addition of Pr [1]. The Pr concentration at grain boundaries was measured via STEM EELS to be approximately three times greater than adjacent grains. Thus it is believed that the modification of grain boundary electrical properties is related to the population and depopulation of a bandgap electronic state associated with the Pr *4f* level [2] localized to within 2 nm – 3 nm of the boundaries. To elucidate the nature of this bandgap state, here we employ monochromated valence-loss EELS using a Nion UltraSTEM to spatially map—and correlate with composition—the position and occupancy of the Pr *4f* level at grain boundaries in $Pr_xCe_{1-x}O_{2-\delta}$.

We have developed an ultra-high energy resolution valence-loss EELS approach to detect and interpret quantitatively the bandgap state associated with the Pr *4f* level in $Pr_{0.1}Ce_{0.9}O_{2-\delta}$ nanoparticles [3]. As shown in fig. 1a, valence-loss spectra included a plateau feature at approximately 1.4 eV – 3.2 eV, attributed to electronic transitions from the O *2p* valence band into Pr *4f* levels in the bandgap of CeO_2 [2]. The conduction band onset at 3.2 eV corresponds to valence-to-conduction band transitions from O *2p* to Ce *4f* levels. To interpret the valence-loss spectra, the EELS single-scattering distribution, overlaid in fig. 1a, was computed via a joint density-of-states (DOS) approximation described by Egerton [4]. This enabled us to replicate the experimentally determined valence-loss data by systematically varying the position and intensity of Pr *4f* DOS relative to computed CeO_2 DOS data from literature, fig. 1b. The bandgap Pr 4f state is treated as a sharp Gaussian function centered approximately 1.4 eV above the O *2p* valence band maximum (i.e. 0 eV in fig. 1b). Another interesting result of this work was that the ratio of Ce and Pr *4f* DOS used to compute the single-scattering distribution was approximately that of the material's nominal composition, suggesting that this technique may also be useful for assessing composition as well as electronic structure.

In this contribution we extend this approach to map the Pr *4f* bandgap state in the vicinity of grain boundaries in $Pr_xCe_{1-x}O_{2-\delta}$ polycrystalline thin films grown via pulsed laser deposition (PLD). Ceria-based PLD thin films, e.g. fig. 2a, can exhibit small columnar grains with relatively high grain boundary density, and grains that are crystallographically oriented with the film substrate. Many grain boundaries are thus highly oriented, as in fig. 2b, yielding ideal conditions for (S)TEM study. Furthermore, we can modify the Pr enrichment of the boundary through variation of the nominal film composition (i.e. *x* in $Pr_xCe_{1-x}O_{2-\delta}$), which is confirmed via core-loss EELS. In this way we can observe the influence of nominal and boundary composition on the intensity of the Pr *4f* bandgap state relative to the Ce *4f* level, providing key materials science insights related to charge transport. Technique development goals include determination of the sensitivity and spatial resolution of this bandgap state mapping approach, especially elucidation of the impact of signal delocalization. [5]

References:

[1] W.J. Bowman, J. Zhu, R. Sharma and P.A. Crozier, Solid State Ionics **272** (2015), 9.

[2] J.J. Kim, S.R. Bishop, N.J. Thompson, D. Chen, *et al.*, Chem. of Mater. **26** (2014), 1374.
[3] W.J. Bowman, K. March, C.A. Hernandez, P.A. Crozier, Under Review (2016).
[4] R.F. Egerton, Electron Energy-Loss Spectroscopy in the Electron Microscope (Springer, New York, 2011), Ed. 3, p. 206.
[5] W.J.B. was a Swiss Government Excellence Scholarship holder for the academic year 2015-2016 (ESKAS 2015.1183), and acknowledges financial support of the US NSF Graduate Research Fellowship Program (grant DGE-1311230), the NSF Graduate Research Opportunities Worldwide grant, and NSF DMR-1308085.

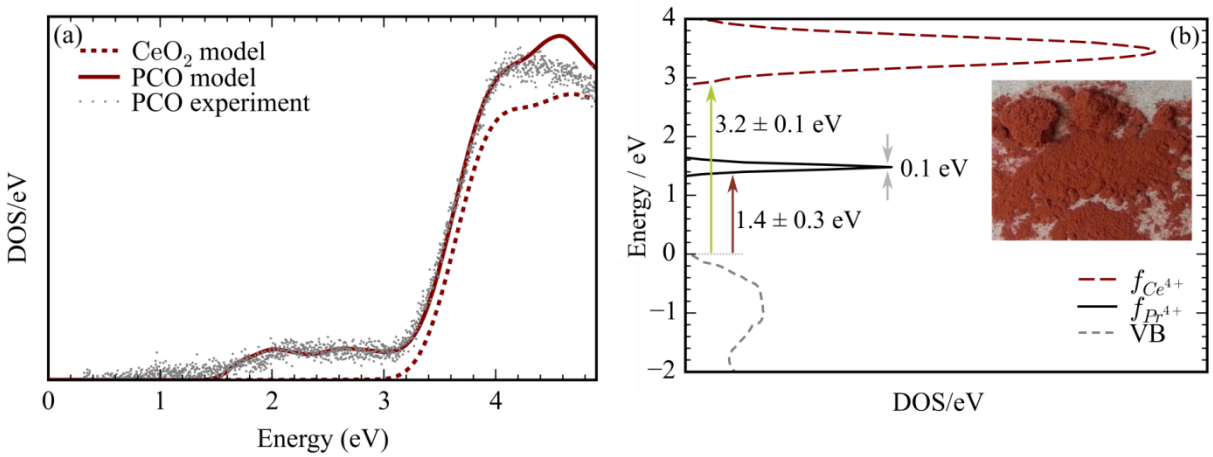

Figure 1. (a) Single-scattering distributions calculated for model CeO_2 and PCO, with measured PCO EELS [3]. (b) DOS for PCO showing valence-to-conduction and valence-to-impurity transitions (labelled arrows). Inset is an image of PCO nnaoparticles following heating in air, whereby particles are assumed stoichiometric, with Pr 4f impurity band unoccupied [3]. 0 eV represents the valence band maximum.

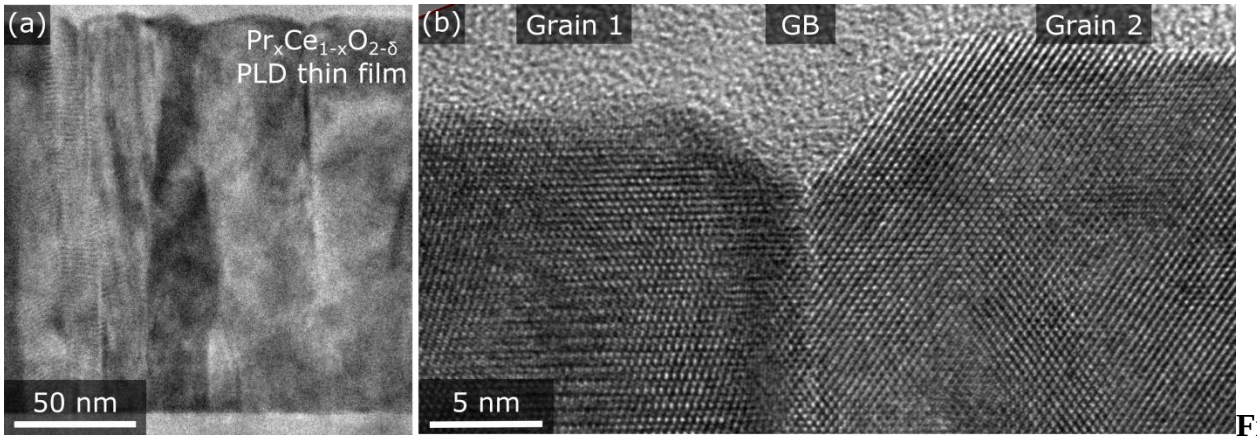

Figure 2. (a) Representative PLD thin film microstructure and (b) atomic resolution image of grain boundary (film courtesy of Sean Bishop). The localization and character of the Pr *4f* bandgap state will be investigated at similar grain boundaries.

https://doi.org/10.1017/S1431927616005699 Published online by Cambridge University Press